Microbiological influence of metal ion electrodeposition: studies using graphite electrodes, $[AuCl_4]^-$ and *Shewanella putrefaciens*

Jeet Varia[a], Susana Silva Martinez, Sharon Velasquez-Orta, Steve Bull
School of Chemical Engineering and Advanced Materials, Newcastle University, Newcastle upon Tyne, Tyne and Wear NE1 7RU
[a] Corresponding author: E-mail address : jeet.varia2@ncl.ac.uk

Abstract

The microbiological influence of gram negative dissimilative bacteria on the electrodeposition of gold $[AuCl_4]^-$ ion is analysed. Previous investigations have shown positive shifts in revisable potentials of gold electrodeposition with 1×10^{10} CFU ml^{-1} of *Shewanella Putrefaciens* in the electrolyte bath. We analyse the hypothetical influences of bacterial cells on gold nucleation and electrodeposition reaction mechanisms, kinetics and mass transfer as a basis for further investigation and strategies for the engineering of robust bioelectrochemical systems for novel metal ions recovery from aqueous process streams.

1. Introduction

The interactions of microbiological bacterial cells and electrified interfaces, termed bioelectrochemical systems (BES) have been well documented over the last 20 years [1], with a great deal of interest in their application for recalcitrant wastewater remediation using microbial fuel cells and microbial electrolysis cell [2]. The processes here, involve the reciprocal alliance of microbial cells and electrochemical systems for inorganic wastewater remediation [3, 4]; with microbial biosorption coupled with the sustenance of bacterial cells, by direct (DET) or mediated (MET) [5, 6] electron transfer to microbial cells. Inorganic contaminants are simultaneously reduced in the final step of the biosorption mechanism [7, 8], as their role as final electron acceptors for bacterial respiration [9, 10] leads to the remediation of inorganic contaminated wastewater [3, 4].

The coupling of biological remediation of inorganic contaminated water with proton reduction or direct electron transfer at electrified interfaces has shown some promise [4, 6, 11, 12]. Thus, the possibility of the cathodic biocatalysis [13] of metal reduction and deposition, by biological protein enzymes located on the bacterial cell wall, or released by bacterial cells [14, 15] could be another alternative bio-electrochemical metal ion remediation strategy. Where bacterial cells influence metal ion electron transfer thermodynamics, kinetics and metal ion mass transfer, leading to their remediation and recovery, with perspective reduction in energy and/or time. This coupled with the simultaneous biosorption and recovery of metals by live and/or deactivated bacterial cells [16, 17] leading to, in principle, a versatile remediation and recovery methodology.

The work presented here aims to further add upon preliminary investigations [18], and further the unabridged aims of the overall research to develop strategies for the cleaning of metal contaminated aqueous systems such as mine waters or industrial effluents, characterised with low metal ions concentration (< 200 ppm) and low pH (< 3), to acceptable regulatory levels, by the symbiotic coupling of microbiological and electrochemical phenomena. *Shewanella putrefaciens,* chosen as an atypical electroactive chemolipothropic gram negative bacterium [19], which biosorbs a range of metal ions [9, 20-25], and exhibit some application within BES [26]. With perspective for the recovery of the metal contaminant [27] in a form applicable for reuse. Such application of bacterial cell walls as “bio-nano-factories” can lead to the manufacture of biogenic nanoparticles [21, 22, 28-30] and possible enhancement or novel microbial influence on metal ion nucleation and deposition phenomena. The processes are developed within specified boundaries of green chemistry principals, carried out at ambient conditions with no further addition of chemicals, to be commercially, sustainable and viable [31].

Following on from previous report of bacterial influence on electronation thermodynamics of Au^{3+}, Co^{2+} and Fe^{3+} ions [18] this manuscript gives further analysis and modelling of the data and provides electrochemical experimentation with 200 ppm $AuCl^{4-}$ electrolytes pH 2, graphite grade G-10 electrodes and bacterial cells. With analysis of theoretical bacterial influence upon gold electrodeposition kinetics, mass transfer and electronucleation phenomena, further understanding of the bacterial influence through theoretical modelling. Fig. 1 summarises hypothetical biological mediated routes for their strategic technological application.

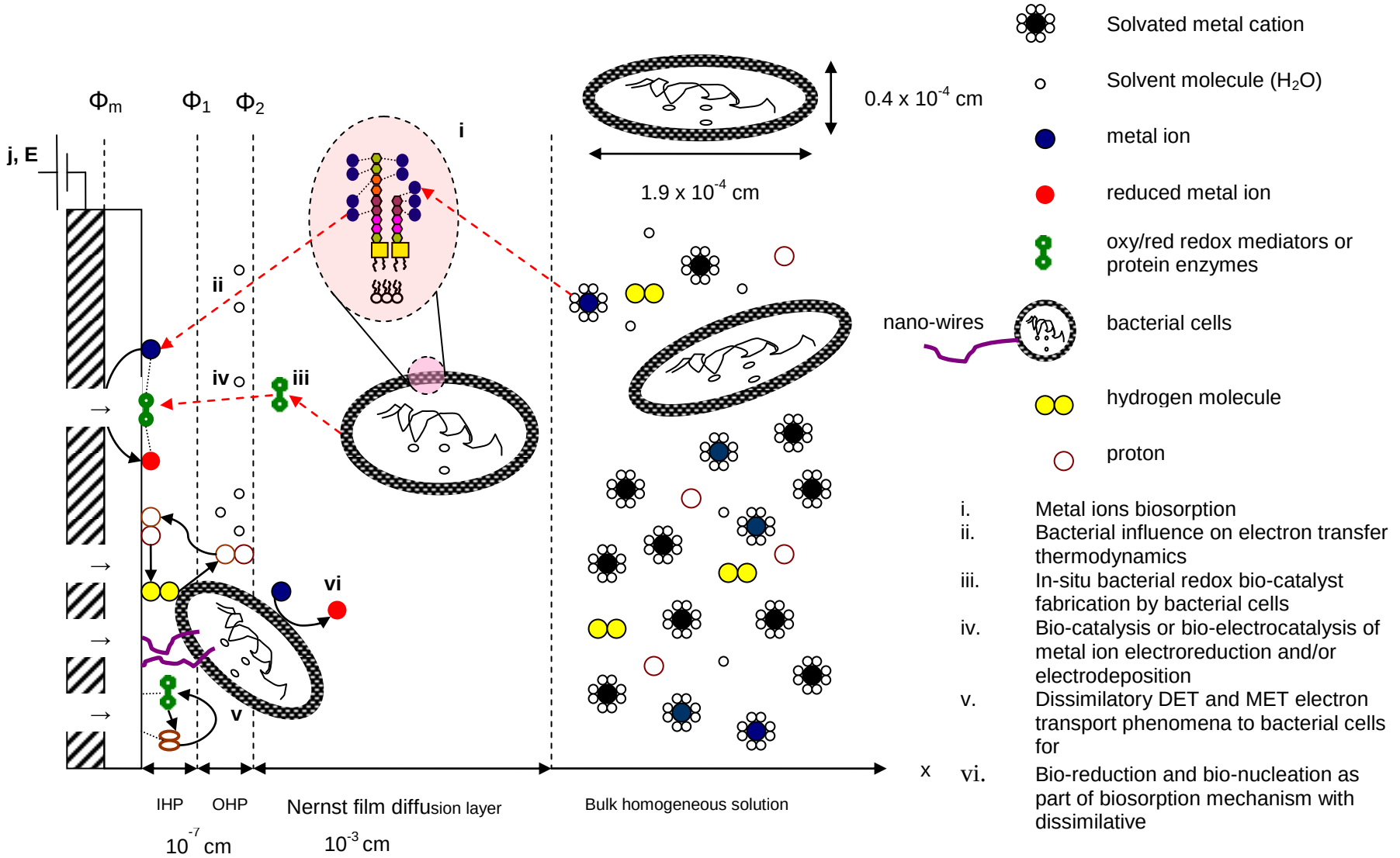

Figure 1 : Bio-electrochemical metal ion remediation interface (IHP – inner Helmholtz plane, OHP – outer Helmholtz plane) [16].

2. Experimental

2.1. Materials and Methods

Aqueous electrolyte solutions of 200 ppm Au^{3+} were prepared with 1000 ppm standard solutions of $HAuCl_4$ in 2 M HCl base electrolyte matrix. The pH of electrolytes was adjusted with NaOH or HNO_3, with final conductivities of electrolytes for gold, 32.5 mS cm^{-1}. Solutions were prepared from analytical grade reagents supplied by Fisher Scientific International Company or standard solutions from Spectrosol (VWR). Triple distilled water was used to prepare all solutions. Details of apparatus, experimental set up, microbial strain, medium and cultivation can be found elsewhere [18]. All potentials are reported with respect to an Ag/AgCl reference electrode.

3. Results and Discussion

The overall reaction for gold electrodeposition from chloride solutions can be described by Eq. (1).

$$AuCl_4^- + 3e^- \rightarrow Au^0 + 4Cl^- \qquad (1)$$

With previous reports of a reaction mechanism involving two charge transfer steps with a preceding chemical step (c.e.e. mechanism) [32-34], described by Eq. (2a-2c) [33]. Tafel analysis of *Log(j) vs. E* for relatively small overpotentials (η) > 0.1 V can be applied for the inference of the rate determine step (RDS) and reaction kinetics [35]. Where *j* is the current density and *E* is the overpotential. Tafel slopes (λ) of 120, 60 and 25 V dec^{-1} would correlate to reaction steps (2a), (2b) or (2c) being the rate determining step (RDS), of the overall reaction mechanism [35, 36].

$$[AuCl_4]^- \rightarrow [AuCl_3]^+_{(ads)} + 2Cl^- \qquad (2a)$$
$$[AuCl_3]^+_{(ads)} + 2e^- \rightarrow [AuCl_2]^-_{(ads)} \qquad (2b)$$
$$[AuCl_2]^-_{(ads)} + e^- \rightarrow Au^0 + 2Cl^- \qquad (2c)$$

Furthermore, the exchange current density (j_0) can be used as an indicator of microbial influence on reaction kinetics of gold electrodeposition [37]. An increase in j_0 would be indicative of faster reaction kinetics. Table 1 summarises the parameters obtained from linear fits of Tafel plots for overpotentials of -0.025 V to -0.075 V illustrated by Fig. 2, without (a) and with bacterial cells (b). Tafel analysis using a Pt electrode is also included in Table 1, as a basis for further comparison with graphite electrodes.

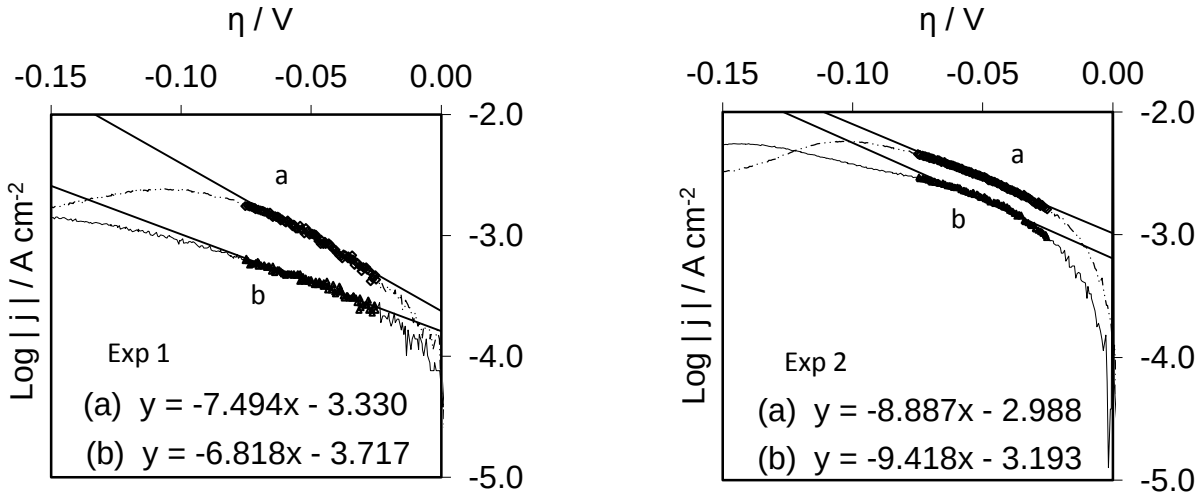

Figure 2 : Tafel plots for Au^{3+} electrodeposition (scan rate = 0.010 V s^{-1}) on an G10 graphite electrode at 25°C from 200 ppm Au^{3+} in 2 M HCl matrix pH = 2, κ = 35.2 mS cm^{-1}, (a) without bacterial cells (b) with 10 ml 1x10^{10} CFU ml^{-1} bacterial cells. The polarisations were carried out 10 minutes after the addition of bacterial cells.

Table 1 : Reversible potentials (E_r), Tafel slopes (λ) and exchange current density (j_o) determined from slow scan (0.010 V s^{-1}) linear voltammetry.

		E_r / V *vs*. Ag/AgCl		λ / V dec^{-1}		j_o x 10^{-5} / A cm^{-2}		
	Exp.	a	b	a	b	a	b	% change
Pt Electrode		0.647	-	0.059	-	5.61	-	
Graphite	1*	0.618	0.749	0.133	0.147	46.83	19.20	-59%
Grade 10	2**	0.660	0.708	0.113	0.106	102.83	64.15	-38%
	Avg	0.639	0.729	0.123	0.126	74.826	41.677	-44%
	SD	0.030	0.029	0.015	0.029	39.597	31.782	

*[18], ** This study

Reversible potentials (E_r) for Exp 2 in the presence of bacterial cells, show a positive shift in reversible potentials as reported previously [18]. A Tafel slope of 0.059 V dec^{-1} for Pt electrode, would suggest an electron transfer step Eq. (2b) to be rate controlling [33]. Higher Tafel slopes are found when graphite was used since Tafel slopes of 0.133 and 0.112 V dec^{-1} would suggest $AuCl_3^-$ adsorption described by Eq. (2a), to be the rate determining step. For scans with bacterial cells a deviation is seen which would imply bacterial influence on reaction mechanisms. Although dissimilar variation is revealed, this work does show some bacterial influence.

A reduction in the j_o is also noted and indicative of bacteria lag of electron transfer kinetics. If based on Tafel analysis, reaction Eq. (2a) is the RDS, bacteria appear to hinder adsorption of gold ions to the electrode surface. Eq. (3) gives a more comprehensive definition of j_o [35] where $\Delta G^{0\#}$ is the Gibbs free energy of activation, h is the Planck Constant, k_B is the Bolzmann constant and α_c transfer coefficient [36]. A reduction of j_o would indicate that bacterial cells or bacterial components increase $\Delta G^{0\#}$ of election transfer to gold metal ions located in the IHL. $\Delta G^{0\#}$ can be further defined by Eq. (4), which would imply that bacteria increase or decrease activation enthalpy or entropy respectively.

$$j_o = \frac{k_B T}{h} F C_i \left[exp \frac{-\alpha_c F \Delta\varphi_e}{RT} \right] \left[exp \frac{-\Delta G^{0\#}}{RT} \right] \qquad (3)$$

$$\Delta G^{0\#} = \Delta H^{0\#} - T\Delta S^{0\#} \qquad (4)$$

Further linear voltammograms under potentiodynamic conditions were carried out to further infer of the system at hand. Fig. 3 illustrates a set of linear voltammograms with varying scan rates (0.010 – 0.120 V s^{-1}). After each scan the electrolyte was stirred with a magnetic stirrer and the working electrode polarised at a potential of +1.00 V vs. Ag/AgCl until initial OCP was re-established [18].

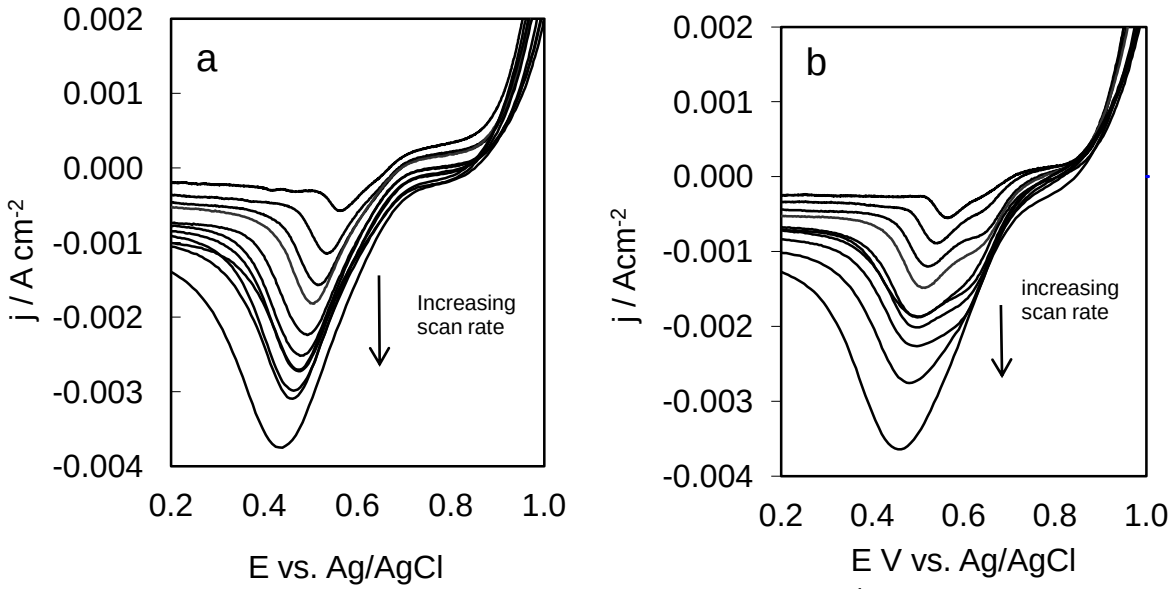

Figure 3 : Set of linear voltammograms for Au^{3+} (0.010 – 0.120 V s^{-1}) on grade G10 graphite electrode at 25°C from 200 ppm Au^{3+} in 2 M HCl matrix, pH = 2, κ = 35.2 mS cm^{-1}. The voltammograms were carried out 10 minutes after the addition of bacterial cells, (a) without bacterial cells, (b) with 10 ml 1x10^{10} CFU ml^{-1} bacterial cells.

Both systems show that the foot of the cathodic peak is steep, implying that nucleation of the metal phase is followed by rapid nuclei growth [38], peak potential (E_p) shifts negatively with increasing the scan rate (S) which would be most likely due to an increase in the nucleation overpotential with S. Furthermore, E_p is proportional to $S^{1/2}$ (Fig. 4) modelled using linear fitting, which would suggest that the metal deposition reaction is diffusion controlled [38]. Similar trends are seen for both systems with and without bacterial cells. It is worth to note the change in E_p with respect to $S^{1/2}$, *i.e*. the gradient of the line is lower with bacteria present in the electrolyte bath.

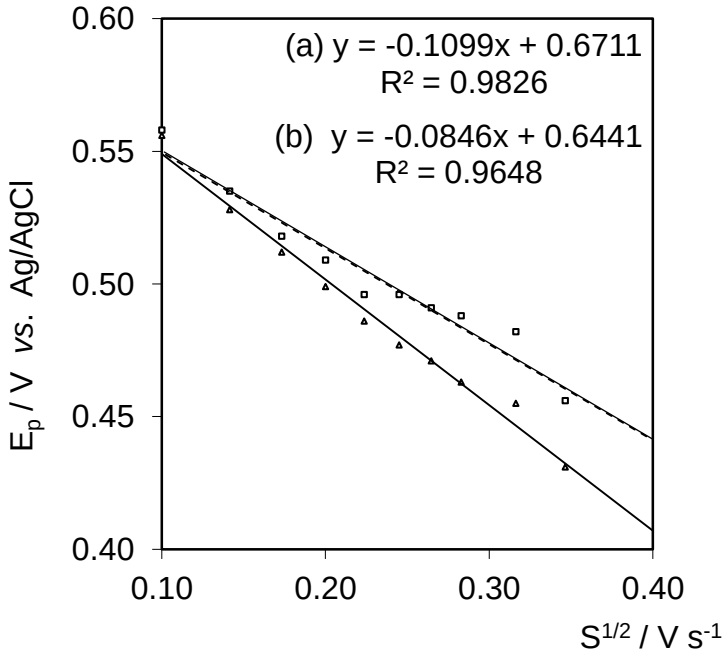

Figure 4 : E_p *vs*. $S^{1/2}$ for gold electrodeposition on grade G-10, (a) without (o symbol) and (b) with 10 ml 1x10^{10} CFU/ml bacterial cells (Δ symbol)).

A linear relationship of peak current density, j_p / A cm^{-2} *vs*. $S^{(1/2)}$, from Fig. 3, would again point to diffusion limited metal nucleation mechanism. Fig. 5 illustrates such a plot, which shows linear correlation and a diffusion-limited process. Linear regression fitting of the data can be used for the determination of metal ion diffusion coefficients $D_{(AuCl4)-}$ using the Randles-Sevcik equation [37], described by Eq. (5). Where C_o is the metal ion concentration and *n* is the number of moles of electrons transferred in the reaction. Linear regression fitting yielded diffusion coefficients D of 1.379 x 10^{-6} and 0.927 x 10^{-6} cm^2 s^{-1} for experiments without (a) and with bacteria cells (b) respectively. A reduction of the diffusion coefficient would suggest that bacteria reduce the mobility of metal ion to the electrified interface.

$$j_p = (2.69 \times 10^5) n^{3/2} C_o D^{1/2} S^{1/2} \qquad (5)$$

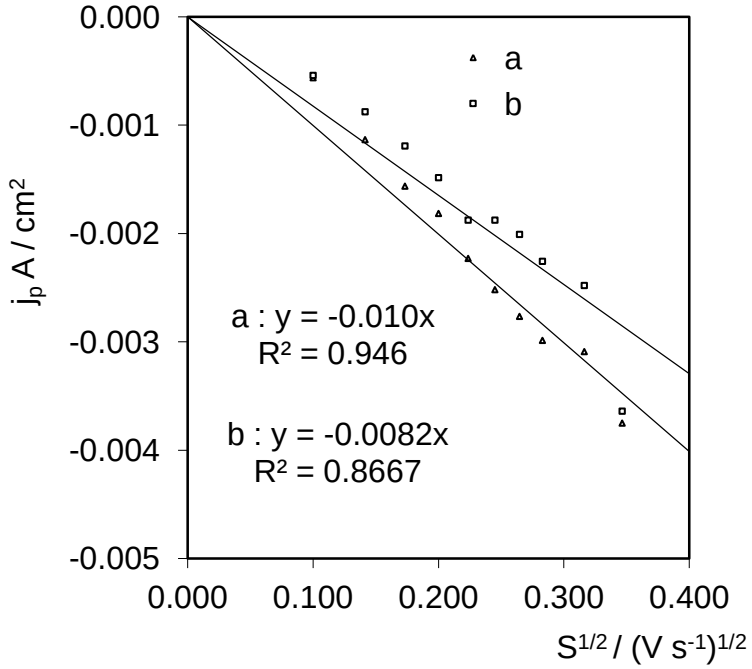

Figure 5 : Randles-Sevcik plot of j_p *vs*. $S^{1/2}$ for gold electrodeposition on grade G-10, (a) without and (b) with 10 ml $1x10^{10}$ CFU/ml bacterial cells.

Fig. 6 illustrates average steady state current densities (j_L) taken after a 60 s potential step, ranging from 0.6 V to -0.2 V vs. Ag/AgCl. On average lower limiting currents are found when bacteria are added to the electrolyte. This would indicate as shown in previous investigations [18] that bacteria hinder diffusion phenomena of metal ions to the electrified interface by the attachment and colonisation of bacterial cells to the electrode for defensive and/or dissimilatory [6] motives.

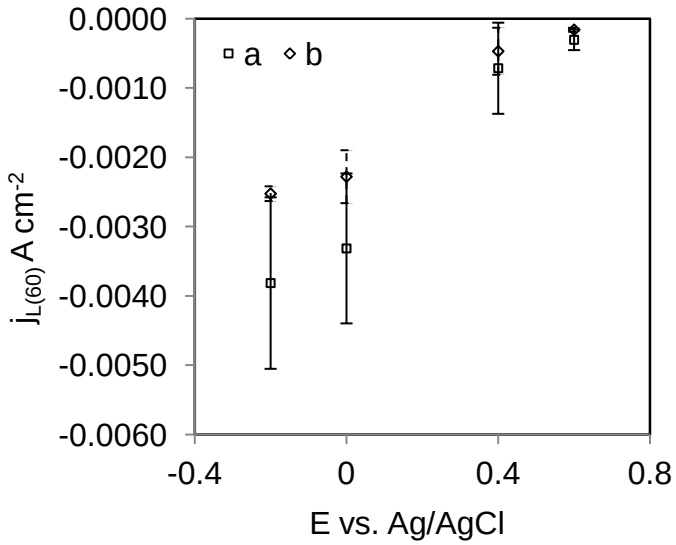

Figure 6. Steady state current density $j_{L(60)}$ vs. E, taken after application 60 seconds potential steps. (a) without bacterial cells, (b) with 10 ml $1x10^{10}$ CFU ml^{-1} bacterial cells (experiment carried out in duplicate), potential step applied after 10 minutes addition of bacterial cells.

The nucleation and growth phenomena in the initial stages of the gold deposition were investigated by chronoamperometric experimentation as extensively applied for analysis of electronucleation [39, 40]. Fig. 7 illustrates the current transients obtained with potential steps of the working electrode of +0.7 to -0.2 V. After each experiment as with cyclic voltammograms a potential of 1.00 V was applied until OCP was re-established (≈ 0.7 V). The transients with potential steps of +0.7 V exhibit an initial current decay (t < 0.001 s) which would be related to double layer charging. A current decay is not seen for other potential steps. A characteristic current increase is shown for all transients (t < 1 s) which would be due to the nucleation and growth of gold nanoparticles on carbon electrode surface. The observed maximum j_M resulting from the overlap of growing particles and diffusion zones [41]. The shape of transients are similar on the whole for both systems without and with bacterial cells (Fig 7), although much higher currents are observed for low potential steps near the E_r of $AuCl_4^-$ with bacteria(Table 1), which reinforces the analysis of slow scan polarisations. Furthermore the shape of the transient for potential steps of 0.6 V are significantly different, with a steeper current decay indicating residual currents involving additional electron transfer reactions, or higher rates of gold nucleation. A higher current maximum j_M and corresponding time maximum t_M with bacterial cells in the electrolyte is also observed.

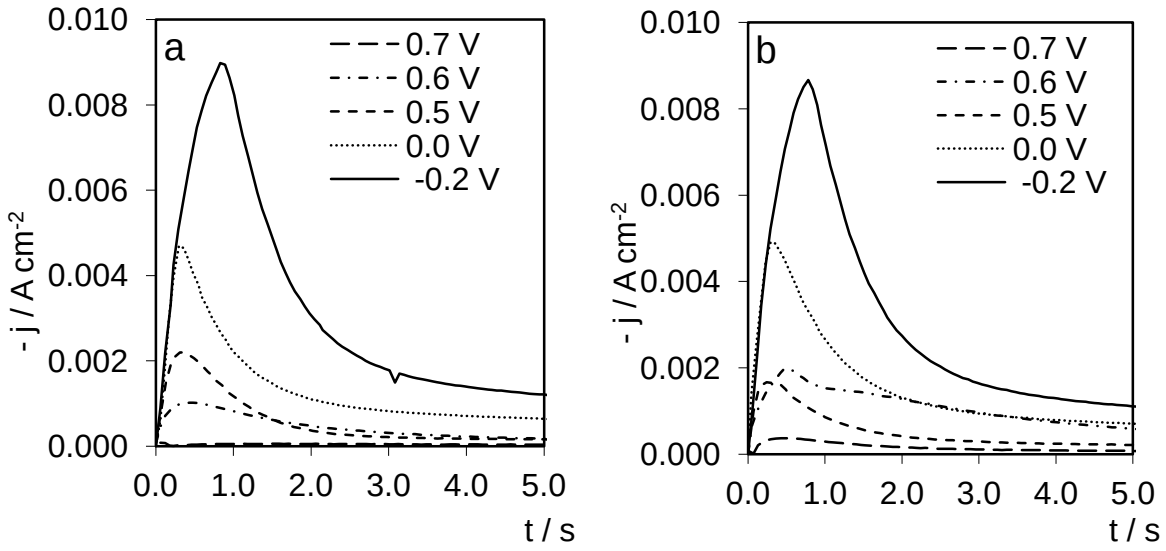

Figure 7 : Current-time transients for nucleation of gold on graphite carbon for various potential steps, (a) without bacterial cells, (b) with 10 ml 1x10^{10} CFU ml^{-1} bacterial cells. Polarisations were carried out 10 minutes addition of bacterial cells.

The decreasing part of the transients traced in the coordinates of j vs. $t^{-1/2}$, define a straight line (Fig. 8) and the diffusion coefficients can be estimated by application of the Cottrell equation (Eq. 6).

$$j = -\frac{nFD^{1/2}C_o}{\pi^{1/2}t^{1/2}} \qquad (6)$$

Table 2, summaries calculated diffusion coefficients for potential range from 0.6 V to -0.2 V. The average value is shown to be significantly higher to that calculated using the Randles-Sevcik equation (0.1379x10^{-5} and 0.0927x10^{-5} $cm^2\ s^{-1}$

without (a) and with bacteria cells (b) respectively). As discussed previously, for potential steps of 0.6 V, with bacteria in the electrolyte (Fig. 8b), a change in the shape of the current time transient is shown for initial current increase and later current decay. This from the Cottrell equation is observed, with an increasing slope of residual cathodic current. This would suggest bacterial redox active enzymes are of active influence close to these potentials, and involved in electron transfer close to onset potentials of the electrodeposition process.

Table 2. Diffusion coefficient (D) calculated from the Cottrell (Eq. (6) and Fig. 8). (a) without bacterial cells, and (b) with 10 ml 1x10^{10} CFU ml^{-1} bacterial cells.

	E vs. Ag/AgCl					
	0.60	0.50	0.00	-0.20		
	D / cm s^{-1} x 10^{-5}					
					Average	SD
(a)	0.15	0.58	8.18	22.73	7.91	4.52
(b)	n/a	0.91	10.51	17.60	9.67	6.79

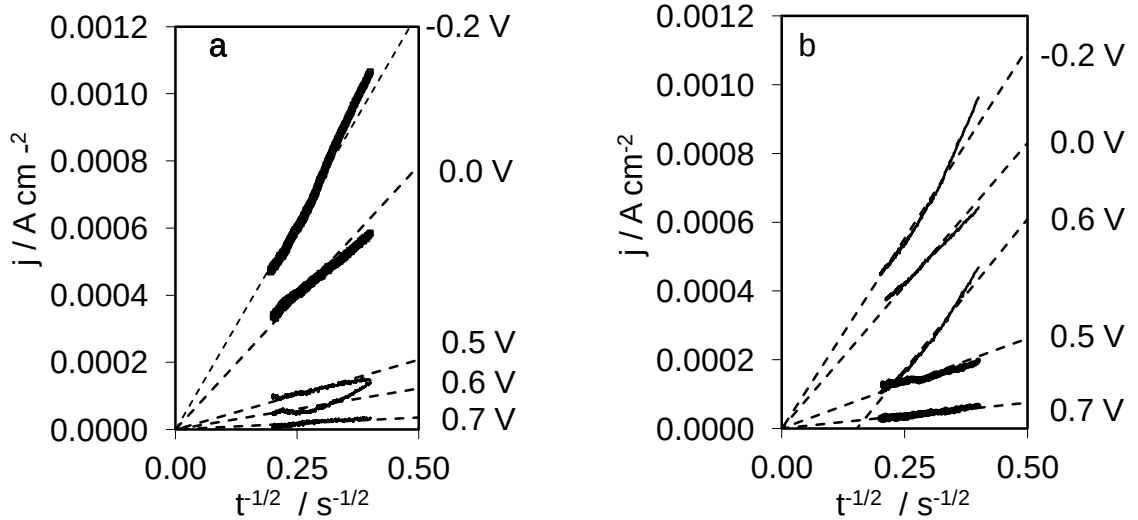

Figure 8. j vs. $t^{-1/2}$ plot from data of transients for nucleation of gold on graphite carbon for various potential steps, (a) without bacterial cells, (b) with 10 ml 1x10^{10} CFU ml^{-1} bacterial cells. Polarisations were carried out 10 minutes addition of bacterial cells.

Potentiodynamic cyclic voltammetry analysis described a diffusion controlled mechanism, and in light of the graphite substrates, usually having a large number of 3D defects (e.g pores and steps) [40]. A 3D, diffusion control model based on investigations by Scharifker and Hills (SH) [42] has been applied extensively [39] and has been utilized here for a simple diagnostic test for the determination of nucleation and growth type and possible influence of bacterial cells. Three dimensional nucleation under diffusion control can be determined from experimentally measured current transients and reduced to non-dimensional form by

plotting j^2/j^2_m versus $(t/t_m)^2$, where j_m and t_m relate to minimum current density and time measurements from the chronoamperometric polarisations, depicted in Fig. 9. In accord with the SH model, the rising current would correspond to an increase in electroactive area. This increase in electroactive area might be limited by spherical diffusion around the nuclei due to an increase in the (a) nucleus size and (b) increase in the number of nuclei sites. As the nuclei grows, spherical diffusional zones overlap mass transfer thereon becomes linear to the planer surface. A basic dichotomy of instantaneous or progressive nucleation can be quantitated relating to nucleation rates.

Instantaneous nucleation relates to high nucleation rate, where all nuclei are immediately created upon application of overpotential, their number remains constant during the growth process, as described by Eq. (7).

$$j = \frac{zFD^{1/2}}{\pi^{1/2}t^{1/2}}\left[1-\exp\left(-N\pi kDt\right)\right] \qquad (7)$$

Where z = 3, F is the Faraday constant (96, 500 C mol^{-1}), C is the $[AuCl_4]^-$ concentration (1.015 x 10^{-6} mol cm^{-3}), N is the density of nuclei (cm^{-2}), and k is the material constant, calculated using Eq. (8).

$$k = \left(\frac{8\pi CM}{\rho}\right)^{1/2} \qquad (8)$$

Where M is the atomic weight of Au (196.97 g mol^{-1}) and ρ is the density of Au (19.30 g cm^{-3}).

The opposing case of progressive nucleation relates to a low nucleation rate, where nuclei are continuously formed and can be described by Eq. (9).

$$j = \frac{zFD^{1/2}}{\pi^{1/2}t^{1/2}}\left[1-\exp\left(\frac{-AN_0\pi k' Dt^2}{2}\right)\right] \qquad (9),$$

where k' is the respective material constant described by Eq. (10), N_o is the density of active nucleation sites (cm^{-2}) and A is the nucleation rate constant (s^{-1}).

$$k' = \frac{4}{3}\left(\frac{8\pi cM}{\rho}\right)^{1/2} \qquad (10),$$

Qualitative characterisation of nucleation process can be determined by plotting current transients described by Eq. (11) and (12) for instantaneous and progressive nucleation, respectively. If transients are found to fall in either of these limiting cases, further quantification of nucleation parameters can be determined.

$$\frac{j^2}{j_m^2} = \frac{1.9542}{t/t_m}\left[1-exp\left(-1.2564(t/t_m)\right)\right]^2 \qquad (11),$$

$$\frac{j^2}{j_m^2} = \frac{1.2254}{t/t_m}\left[1-exp\left(-2.3367(t/t_m)^2\right)\right]^2 \qquad (12).$$

SM fitting for 0.6 V potentials described by Fig. (7), without bacteria show initial instantaneous mechanism which becomes progressive after the current maximum. For electrolytes with bacteria, initially a progressive mechanism is observed

becoming instantaneous after current maximum. The change from instantaneous to progressive is significantly rapid when bacteria are added to the electrolyte. The opposite effect is observed for potentials of 0.5 V, with the transient after current maximum becoming progressive for systems without bacterial cells and moving from instantaneous to progressive for systems with bacterial cells. The initial rising transient shows no correlation to either limiting case. For low potentials of 0.0 V and -0.2 V SH curve fittings show good correlation to progressive nucleation models for $t < t_m$ for systems with and without bacterial cells. For a progressive reaction mechanism, the product AN_0 can be calculated using Eq. (13).

$$j_m = 0.4615zFcD^{3/4}(k'AN_0)^{1/4} \qquad (13),$$

While, the diffusion coefficient can be estimated from Eq. (14),

$$j_m^2 t_m = 0.2598D(zFc)^2 \qquad (14),$$

and the nuclei saturation N_s (cm^{-2}) can be determined from Eq. (15) ,

$$N_s = \left(\frac{AN_0}{2k'D}\right)^{1/2} \qquad (15)$$

Table 3 summarises key values extracted from Fig. 9 for potential steps from 0 V vs. Ag/AgCl, and calculated parameters of *ANo*, *D* and N_s using Eq. (13) and (15). Based on applied theoretical modelling, bacteria show some, although not significant lagging of electrodeposition kinetics, with a decrease in AN_0 also observed from Tafel analysis. It is observed an increase in mobility of metal ions in their journey to the electrified interface with 20% increase of the diffusion coefficient. Contradictory to analysis of metal deposition limiting currents and Cottrell plots. A 40% decrease in the nuclei saturation N_s was also found for electrolytes with bacteria, indicating a lower number of nucleation sites in their presence.

Table 3 : Characteristic parameters of j *vs*. t transients for potential steps to 0.0 V *vs.* Ag/AgCl on graphite G-10 and calculated AN_o, N_s for 3D progressive nucleation. (a) without bacterial cells, (b) with 10 ml $1x10^{10}$ CFU ml^{-1} bacterial cells.

	Units	(a)	(b)
E	V *vs*. Ag/AgCl	0.0000	0.0000
t_m	s	0.3000	0.3400
I_m	A	0.0047	0.0049
D x 10^{-5}	cm s^{-1}	29.4900	36.4500
AN_o		2.605 $x10^6$	1.641 $x10^6$
N_s		4.531 $x10^5$	3.234 $x10^5$

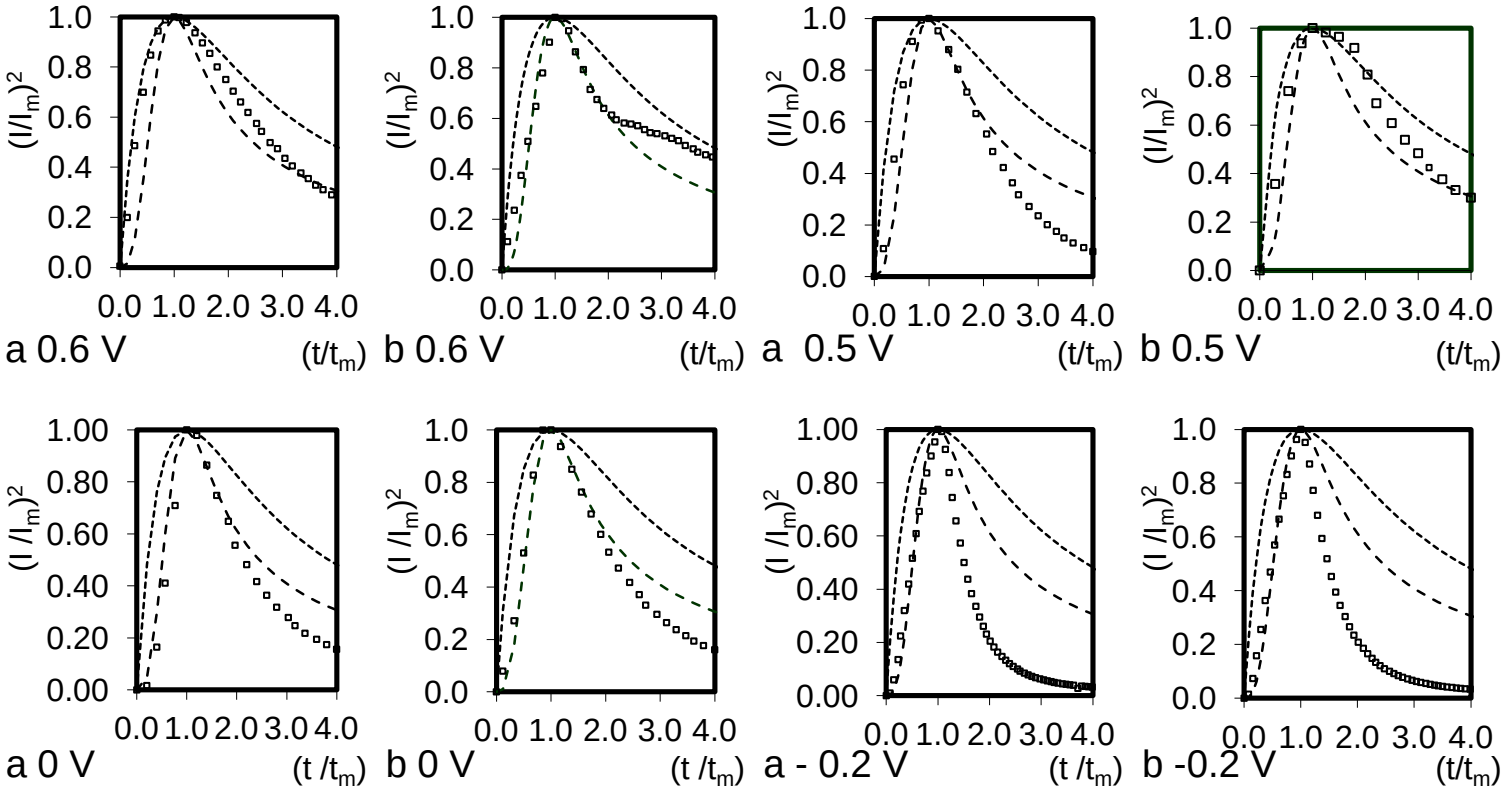

Figure 8 : (j/j_m) vs. (t/t_m) analysis of transient response for Au electrodeposition on graphite grade G-10 for potential steps of 0.6 V to -0.2 V. Together with the data calculated for instantaneous and progressive nucleation, (a) without cells (b) with 10 ml $1x10^{10}$ CFU ml^{-1} bacterial cells for two typical polarisation experimentations. Data (□),theoretical plots for instantaneous (top) (- - -) and progressive (bottom) (---) nucleation.

4. Conclusions

The electrodeposition of gold on grade G-10 graphite electrodes was investigated in the presence of electroactive bacterial cells of the Shewanella genus. This upon previous reports of bacterial influence on electron transfer thermodynamics and hypothesised bacterial enhancement of electron transfer phenomena, with the perspective and strategic alliance of electrochemical and microbiological phenomena, for the remediation and recovery of metal ions. Our results have shown some influence of bacterial cells on reaction mechanism from deviation of Tafel slopes (λ), a lagging of electron transfer kinetics (j_0) and mass transfer kinetics ($j_{(60)}$). Modelling of chronoamperometric transients using 3D, diffusion control model based on investigations by Scharifker and Hills was consistent with these observations. Although further electrochemical and microscopy experimentation and analysis of bacterial influence on electron metal ion transfer reactions is required before conclusive assertions can be made on their influence.

We believe the work here provided some insight into how these may be elucidated. Also further investigation with other bacterial species would be justified, in light of monumental advances in molecular biology, genetics and biochemistry, for the bio-engineering of robust electroactive bacterial cell membranes [43]. Which allow the subsistence of bacterial cells in non-ideal low pH and toxic environments, engineered to over-express implicated bioremediation redox protein enzymes protein/peptides. Found to be sympathetic to electrodeposition and biosorption reaction mechanisms, leading to savings in energy and time of the remediation process. Further scientific investigation at the molecular level of the lipopolysaccaride outer leaf bacterial cell membrane and localized electron transfer redox membrane proteins interaction with metal ions and carbon electrodes would also undoubtedly further their applicable technological advancement.

This work considered the (a) cleaning of metal contaminated waste water and (b) lucrative recovery of biogenic metal material such as metal nanoparticles. Involving the simultaneous metal ion electrodeposition and biosorption in BES, with bacterial respiration by DET or MET at the electrified interface and bacterial enhancement of electrodeposition, would be of some novel technological application for cleaner water and a green method for metal recovery.

References

[1] K. Rabaey, Bioelectrochemical systems : from extracellular electron transfer to biotechnological application, IWA Publishing, London ; New York, 2010.
[2] L. Huang, S. Cheng, G. Chen, Journal of Chemical Technology & Biotechnology, 86 (2011) 481-491.
[3] S. Ghafari, M. Hasan, M.K. Aroua, Bioresource Technology, 99 (2008) 3965-3974.
[4] J.C. Thrash, J.I. Van Trump, K.A. Weber, E. Miller, L.A. Achenbach, J.D. Coates, Environmental Science & Technology, 41 (2007) 1740-1746.
[5] J.C. Thrash, J.D. Coates, Environmental Science & Technology, 42 (2008) 3921-3931.
[6] K.B. Gregory, D.R. Bond, D.R. Lovley, Environmental Microbiology, 6 (2004) 596-604.
[7] F. Veglio, F. Beolchini, Hydrometallurgy, 44 (1997) 301-316.
[8] C. White, S.C. Wilkinson, G.M. Gadd, International Biodeterioration & Biodegradation, 35 (1995) 17-40.
[9] C. Liu, J.M. Zachara, Y.A. Gorby, J.E. Szecsody, C.F. Brown, Environmental Science & Technology, 35 (2001) 1385-1393.
[10] J.R. Lloyd, FEMS Microbiology Reviews, 27 (2003) 411-425.
[11] K.B. Gregory, D.R. Lovley, Environmental Science & Technology, 39 (2005) 8943-8947.
[12] H.I. Park, D.k. Kim, Y.-J. Choi, D. Pak, Process Biochemistry, 40 (2005) 3383-3388.
[13] A. Bergel, D. Féron, A. Mollica, Electrochemistry Communications, 7 (2005) 900-904.
[14] Y.A. Gorby, S. Yanina, J.S. McLean, K.M. Rosso, D. Moyles, A. Dohnalkova, T.J. Beveridge, I.S. Chang, B.H. Kim, K.S. Kim, D.E. Culley, S.B. Reed, M.F. Romine, D.A. Saffarini, E.A. Hill, L. Shi, D.A. Elias, D.W. Kennedy, G. Pinchuk, K. Watanabe, S.i. Ishii, B. Logan, K.H. Nealson, J.K. Fredrickson, Proceedings of the National Academy of Sciences, 103 (2006) 11358-11363.
[15] E. Marsili, D.B. Baron, I.D. Shikhare, D. Coursolle, J.A. Gralnick, D.R. Bond, Proceedings of the National Academy of Sciences, 105 (2008) 3968-3973.
[16] J. Varia, U.o.N.u.T.S.o.C. Engineering, A. Materials, Bio-electrochemical Systems for the Remediation of Metal-ion Effluents, University of Newcastle upon Tyne, 2012.
[17] J. Varia, A. Zegeye, S. Bull, S. Yahaya, S. Roy, Seperation and Purification (Submitted November 2012 (under review)).
[18] J. Varia, S.S. Martínez, S.V. Orta, S. Bull, S. Roy, Electrochimica Acta, 95 (2013) 125-131.
[19] J.K. Fredrickson, M.F. Romine, A.S. Beliaev, J.M. Auchtung, M.E. Driscoll, T.S. Gardner, K.H. Nealson, A.L. Osterman, G. Pinchuk, J.L. Reed, D.A. Rodionov, J.L.M. Rodrigues, D.A. Saffarini, M.H. Serres, A.M. Spormann, I.B. Zhulin, J.M. Tiedje, Nat Rev Micro, 6 (2008) 592-603.
[20] B.B. Mamba, N.P. Dlamini, A.F. Mulaba–Bafubiandi, Physics and Chemistry of the Earth, Parts A/B/C, 34 (2009) 841-849.
[21] Y. Konishi, K. Ohno, N. Saitoh, T. Nomura, S. Nagamine, H. Hishida, Y. Takahashi, T. Uruga, Journal of Biotechnology, 128 (2007) 648-653.
[22] Y. Konishi, T. Tsukiyama, K. Ohno, N. Saitoh, T. Nomura, S. Nagamine, Hydrometallurgy, 81 (2006) 24-29.

[23] Y. Konishi, T. Tsukiyama, T. Tachimi, N. Saitoh, T. Nomura, S. Nagamine, Electrochimica Acta, 53 (2007) 186-192.
[24] J.R. Haas, T.J. Dichristina, R. Wade Jr, Chemical Geology, 180 (2001) 33-54.
[25] S. De Corte, T. Hennebel, S. Verschuere, C. Cuvelier, W. Verstraete, N. Boon, Journal of Chemical Technology & Biotechnology, 86 (2011) 547-553.
[26] H.J. Kim, H.S. Park, M.S. Hyun, I.S. Chang, M. Kim, B.H. Kim, Enzyme and Microbial Technology, 30 (2002) 145-152.
[27] A. Robert U, Resources, Conservation and Recycling, 21 (1997) 145-173.
[28] H. Korbekandi, S. Iravani, S. Abbasi, Critical Reviews in Biotechnology, 29 (2009) 279-306.
[29] T. Hennebel, B. De Gusseme, N. Boon, W. Verstraete, Trends in Biotechnology, 27 (2009) 90-98.
[30] A.K. Suresh, D.A. Pelletier, W. Wang, M.L. Broich, J.-W. Moon, B. Gu, D.P. Allison, D.C. Joy, T.J. Phelps, M.J. Doktycz, Acta Biomaterialia, 7 (2011) 2148-2152.
[31] J.H. Clark, D.J. Macquarrie, Handbook of green chemistry and technology, Blackwell Science, Oxford England ; Malden, MA, 2002.
[32] A.D. Goolsby, D.T. Sawyer, Anal Chem, 40 (1968) 1978-1983.
[33] J.A. Harrison, J. Thompson, Journal of Electroanalytical Chemistry and Interfacial Electrochemistry, 59 (1975) 273-280.
[34] J.E. Anderson, S.M. Sawtelle, Inorganica Chimica Acta, 194 (1992) 171-177.
[35] J.O.M. Bockris, A.K.N. Reddy, Modern electrochemistry : an introduction to an interdisciplinary research, Plenum Press, New York, 1970.
[36] J.O.M. Bockris, Z. Nagy, Journal of Chemical Education, 50 (1973) 839.
[37] G. Southampton Electrochemistry, Instrumental methods in electrochemistry, E. Horwood ; Halsted Press, Chichester; New York, 1985.
[38] D. Pletcher, R.I. Urbina, J Electroanal Chem, 421 (1997) 137-144.
[39] L. Komsiyska, G. Staikov, Electrochimica Acta, 54 (2008) 168-172.
[40] O. Brylev, L. Roué, D. Bélanger, J Electroanal Chem, 581 (2005) 22-30.
[41] G.J. Hills, D.J. Schiffrin, J. Thompson, Electrochimica Acta, 19 (1974) 657-670.
[42] B. Scharifker, G. Hills, Electrochimica Acta, 28 (1983) 879-889.
[43] K. Kuroda, M. Ueda, Current Opinion in Biotechnology, 22 (2011) 427-433.